Using Pretwist to Reduce Power Loss of Bend-Twist Coupled Blades

Stäblein, Alexander; Tibaldi, Carlo; Hansen, Morten Hartvig

Published in:
Proceedings of the 34th Wind Energy Symposium

Link to article, DOI:
10.2514/6.2016-1010

Publication date:
2016

Document Version
Peer reviewed version

Using Pretwist to Reduce Power Loss of Bend-Twist Coupled Blades

Alexander R. Stäblein, Carlo Tibaldi and Morten H. Hansen
Technical University of Denmark, Department of Wind Energy,
Frederiksborgvej 399, 4000 Roskilde, Denmark

January 2016

Abstract

Bend-twist coupling of wind turbine blades is known as a means to reduce the structural loads of the turbine. While the load reduction is desirable, bend-twist coupling also leads to a decrease in the annual energy production of the turbine. The reduction is mainly related to a no longer optimal twist distribution along the blade due to the coupling induced twist. Some of the power loss can be compensated by pretwisting the blade. This paper presents a pretwisting procedure for large blade deflections and investigates the effect of pretwisting on blade geometry, annual energy production, and fatigue load for the DTU 10 MW Reference Wind Turbine. The analysis was carried out by calculating the nonlinear steady state rotor deflection in an uniform inflow over the operational range of the turbine. The steady state power curve together with a Rayleigh wind speed distribution has been used to estimate the annual energy production. The turbine model was then linearised around the steady state and the power spectral density of the blade response, which was computed from transfer functions and the wind speed variations in the frequency domain, was used to estimate the fatigue loads by a spectral method.

1 Introduction

Bend-twist coupling intends to alter the blade response under aerodynamic loads by introducing a coupling between bending and twist of the blade. This coupling links the aerodynamic loads, which induce a bending moment on the blade, with the twist of the blade. The twist of the blade is directly related to the angle of attack and thus the aerodynamic loads. This mechanism, when twisting towards a lower angle of attack, enables the blade to self-alleviate sudden inflow changes, as in gust or turbulent conditions, leading to a reduction in ultimate and fatigue loads. Bend-twist coupling can be achieved either by sweeping the planform of the blade (geometric coupling) or by utilising the anisotropic properties of the blade material (material coupling). Lobitz and Veers [1] report a significant reduction in fatigue damage (20-80%) due to material bend-twist coupling for fixed and variable speed stall controlled, and variable speed pitch controlled rotors. Verelst and Larsen [2] observe a reduction of up to 10 % in the blade root flapwise fatigue for swept blades. While the load reduction is desirable, bend-twist coupling also leads to a slight decrease in the annual energy production (AEP) of the turbine [2, 3, 4]. The reduction is mainly related to a no longer optimal twist distribution along the blade due to the coupling [2]. Lobitz and Veers [1] suggest to compensate for the power loss by pretwisting the blade to adjust for the coupling induced twist. Lobitz and Veers determine the pretwist of the blade by applying the aerodynamic loads of an uncoupled blade to a coupled blade and applying the linear elastic twist as pretwist to the blade. This paper presents a pretwisting procedure that allows for nonlinear blade deflections and investigates how pretwisting improves the power production of bend-twist coupled blades for a range of coupling coefficients. The effect of pretwisting on fatigue loads are also investigated by means of a spectral method.

The analysis was carried out by calculating the nonlinear steady state rotor deflection in an uniform inflow using the aero-servo elastic code HAWCStab2 [5]. Until recently, HAWCStab2 did not allow for the analysis of material coupled blades. A Timoshenko beam formulation that accounts for fully coupled cross section matrices has therefore been derived and implemented [6]. Bend-twist coupling was introduced by means of a coupling coefficient in the cross-sectional stiffness matrix of the blade as proposed by Lobitz and Veers [7]. To mitigate some of the power loss associated with coupled blades, the structural twist of the coupled blade was modified in an iterative procedure to provide the same angle of attack along the blade as the uncoupled blade at a reference inflow speed. The power curve of the turbine was estimated from the steady states of the operational wind speed range and translated into AEP assuming a Rayleigh wind speed distribution with an mean wind speed of 10 m/s. The damage equivalent load was estimated using a frequency approach recently presented by Tibaldi et al. [8].

2 Methods

This section provides an overview how the steady states of wind turbines are calculated and operational data is obtained in the aeroservoelastic tool HAWCStab2. A summary of the beam formulation for anisotropic cross-sectional properties recently implemented in HAWCStab2 is given. The procedure to reduce energy loss in coupled blades by compensating for the coupling induced twist is presented. The methods to obtain the annual energy production and damage equivalent load rate are also outlined.

2.1 Steady State Computation & Operational Data

HAWCStab2 [5, 9, 10] is an aeroservoelastic tool for the calculation of the steady state properties (i.e. nonlinear blade displacements, aerodynamic forces, power, and thrust) of a wind turbine model around an operational point. An operational point is a combination of wind speed, rotational speed and pitch angle. The steady state properties are calculated assuming uniform inflow over the rotor area, neglecting wind shear, yaw, tilt, turbulence, and tower shadow. Effects from gravity are also ignored. These assumptions result in a stationary steady state due to the symmetry of the inflow and loading. The steady state at an operational point is calculated by an outer, aerodynamic and an inner, structural loop. The outer, aerodynamic loop determines the aerodynamic forces based on the blade element momentum theory including tip loss. The inner, structural loop establishes equilibrium between the external aerodynamic and internal elastic forces by a Newton-Raphson algorithm. The iteration is aborted when convergence of the blade tip displacement is reached. A flow-diagram of the steady state computation in HAWCStab2 is shown in Figure 1. The operational data for a given wind speed is obtained by first calculating the rotor speed from the tip speed ratio of the blade under consideration of the upper and lower limits of the rotor speed. The pitch angle is subsequently determined in an optimization routine that maximizes power below rated and limits power above rated.

2.2 Coupled Blade Model

The structure in HAWCStab2 is modelled by two-noded Timoshenko beam elements [9]. The element coordinate system has its origin in the first node of the element at the elastic centre of the section. The third axis of the coordinate system is pointing towards the second node of the element. The other axes of the coordinate system are rotated according to the principle axes of bending, with the first and second axes pointing towards the leading edge and suction side of the blade. The lateral displacements in the cross-sectional plane $u_1(z), u_2(z)$ are third order polynomials of the cross-sectional position z along the length of the beam L. The rotational displacements $\theta_1(z), \theta_2(z)$ around the beam principle axes follow from Timoshenkos assumption

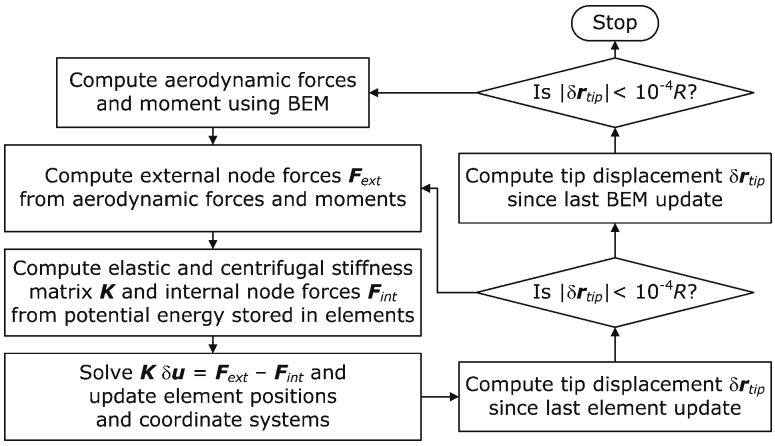

Figure 1: Flowdiagram of steady state computation in HAWCStab2 (Source: The Linear Aero-Servo-Elastic Code HAWCStab2 [11]).

that the rotation of the beam axis equals the slope plus a contribution from shear deformation:

$$\theta_1(z) = -\frac{\partial u_2}{\partial z} + \gamma_x, \qquad \theta_2(z) = \frac{\partial u_1}{\partial z} - \gamma_y \tag{1}$$

First order polynomials are assumed for the longitudinal u_3 and torsional θ_3 displacements. By introducing the beam strain vector

$$\varepsilon = \{\frac{\partial u_1}{\partial z} - \theta_2, \frac{\partial u_2}{\partial z} + \theta_1, \frac{\partial u_3}{\partial z}, \frac{\partial \theta_1}{\partial z}, \frac{\partial \theta_2}{\partial z}, \frac{\partial \theta_3}{\partial z}\}^T \tag{2}$$

and the cross-section stiffness matrix K_{cs} the cross-section constitutive relation is

$$F = K_{cs}\varepsilon \tag{3}$$

where $F = \{F_1, F_2, F_3, M_1, M_2, M_3\}$ are the beam forces and moments in the section. The 14 coefficients resulting from the shape functions of the beam are eliminated by two equilibrium equations

$$\frac{\partial M_1}{\partial z} - F_2 = 0, \qquad \frac{\partial M_2}{\partial z} + F_1 = 0 \tag{4}$$

and 12 compatibility conditions at the element boundaries $z = 0, L$. With the lateral and rotational displacements along the beam determined, the elastic energy V in the beam element is obtained from

$$V = \frac{1}{2}\int_0^L \varepsilon^T K_{cs}\varepsilon \, dz \tag{5}$$

Methods to determine the cross-section stiffness matrix K_{cs} of anisotropic beams have been presented by Giavotto et al. [12] and Hodges [13]. The methods have, for example, been implemented in HANBA2 [12], BECAS [14] and VABS [15].

2.3 Blade Pretwist

The twist and chord distributions of a blade are typically designed to optimize the energy yield at a given tip speed ratio subject to constraints for structural integrity and maximum tip deflection. Under variable speed operation, a blade that has been designed for a specific tip speed ratio is able to maintain an optimal power coefficient over the wind speed range between cut-in and rated. For a blade where bending and torsion is coupled, the twist distribution along the blade depends on the bending curvature of the blade. Between cut-in and rated wind speed, the thrust on the

turbine increases and with it bending and curvature of the blade. A bend-twist coupled blade is therefore not able to maintain the twist distribution required for an optimal power coefficient at a given tip speed ratio. To mitigate some of this bend-twist related power loss the twist distribution of the blade is modified to match the optimal twist distribution at a reference wind speed v_{ref}. For a blade undergoing large displacements and rotations the elastic twist of the blade is not uniquely defined. It can, for example, be measured relative to the local beam axis, the pitch axis of the blade, or a vector perpendicular to the axis of rotation, all of which result in different twist distributions. To allow for nonlinear blade deformations, the twist was measured through the angle of attack. Provided the same wind and rotational speed and similar blade deflections, an equal angle of attack results in the same aerodynamic forces irrespective of the nonlinear blade deformations. The following procedure was used to pretwist the blades:

1. Define reference windspeed v_{ref}.
2. Determine angle of attack α_{ref} of an uncoupled blade at v_{ref}.
3. Calculate angle of attack α_{btc} of bend-twist coupled blade at v_{ref}.
4. Calculate $\Delta\alpha = \alpha_{btc} - \alpha_{ref}$.
5. Add $\Delta\alpha$ to the twist-distribution of the bend-twist coupled blade.
6. Return to 3) and repeat until $\Delta\alpha$ converges to zero.

Once the pretwist at v_{ref} was obtained the pitch angles of the operational points were recalculated as described in Section 2.1 above.

2.4 Annual Energy Production & Damage Equivalent Load Rate

Once the new twist distribution and pitch angles of the blade were determined the steady-state power curve of the turbine was calculated. The power curve was multiplied with a Rayleigh probability density function, assuming a mean velocity of 10 m/s, and integrated to obtain the AEP.

The damage equivalent load was estimated with a frequency-based method proposed by Tibaldi et al. [8]. For each wind speed, the wind inputs $\mathbf{U}_w(\omega)$ in frequency domain along the blades are obtained from sampling of a time domain simulation in HAWC2 [16]. The turbine response $\mathbf{Y}_{gf}(\omega)$ in the ground-fixed reference frame is obtained by joining the wind inputs $\mathbf{U}_w(\omega)$ with the transfer function $\mathbf{H}_{ase}(\omega)$ of the linear aeroservoelastic turbine model from HAWCStab2 between wind inputs and turbine response:

$$\mathbf{Y}_{gf}(\omega) = \mathbf{H}_{ase}(\omega)\mathbf{U}_w(\omega) \tag{6}$$

The blade response $\mathbf{Y}_{bf}(\omega)$ is obtained by a Coleman transformation of the turbine response in the ground-fixed reference frame $\mathbf{Y}_{gf}(\omega)$. Finally, the spectral method proposed by Benasciutti and Tovo [17, 18] is used to determine the damage equivalent load rate for each wind speed from the power spectral density of the blade response $\mathbf{Y}_{bf}(\omega)$. As with the annual energy production, the damage equivalent load rates at each wind speed were weighted with a Rayleigh distribution to obtain an annual damage equivalent load rate.

3 Results & Discussion

To investigate the effect of pretwisting on annual energy production and damage equivalent load rate of bend-twist coupled blades, the methods described in the previous section were applied to the DTU 10 MW Reference Wind Turbine [19]. The reference turbine is a horizontal axis, variable pitch, variable speed wind turbine with a rotor diameter of 178 m and a hub height of 119 m.

The structural properties of the blades in terms of 6x6 cross-section stiffness matrices for application in the anisotropic beam element in HAWCStab2 were obtained with BECAS and

the input data provided on the DTU 10 MW RWT Project Site [20]. Bend-twist coupling was introduced by means of a coupling coefficient γ as proposed by Lobitz and Veers [7]. For a given coupling coefficient γ the entry K_{46} of the cross-section stiffness matrix, which couples flapwise bending with torsion, was obtained as

$$K_{46} = \gamma\sqrt{K_{44}K_{66}} \tag{7}$$

where K_{44} and K_{66} are flapwise bending stiffness and torsional stiffness of the cross-section respectively. For this study, coupling coefficients in the range of $-0.2 \leq \gamma \leq 0.05$ were investigated. Negative values of γ lead to a reduction of the angle of attack for flapwise deflection towards the suction side (twist to feather) while positive values denote twist to stall. The coupling coefficient were assumed constant along the blade.

3.1 Pretwist

The effect of coupling and pretwist on the angle of attack, the twist and the pitch angle of the blade were investigated first. The coupling coefficient was taken as $\gamma = -0.2$ (pitch to feather) and the pretwist reference speed was 8 m/s.

Figure 2 shows the angle of attack along the blade at 8 m/s wind speed for the uncoupled reference blade (green), the coupled blade with the original pitch angle (cyan), the coupled blade with an optimized pitch angle (blue) and the coupled blade with pretwist at 8 m/s (red). The coupling leads to a reduction in the angle of attack along the blade as it twists towards feather. To maximize C_P the coupled blade can be pitched towards a larger angle of attack. However, this does not change the twist distribution along the blade. For a pretwisted blade the angle of attack along the blade is the same as for the reference configuration, resulting in equal aerodynamic forces. Figure 3 shows the angle of attack along the four blades at 7 m/s wind speed. Below the reference speed the thrust on the blades is lower than at reference speed. The lower thrust leads to a reduction of the flapwise moments in the blade and less coupling induced twist. Therefore, the coupled blades twist towards stall compared to reference speed resulting in a larger angle of attack slope with respect to the radial position as shown in the figure. Figure 4 shows the angle of attack along the four blades at 9 m/s wind speed. Above reference speed the thrust on the blades is larger than at reference speed. The larger thrust leads to an increase of the flapwise moments in the blade and more coupling induced twist. Therefore, the coupled blades twist towards feather compared to reference speed resulting in a smaller angle of attack slope with respect to the radial position as shown in the figure.

Figure 5 shows the twist distribution along the blade for the reference blade (green) and the pretwisted blade (red). The figure shows how the pretwist is distributed along the blade to compensate for the coupling induced twist. In the inner third of the blade the twist distributions of the reference and pretwisted blades are nearly equal. Even though coupling has been introduced along the full length of the blade, it has little effect on the twist in this region. In the outer two thirds of the blade the twist of the pretwisted blade increases nearly linearly compared to the reference blade.

To understand why the induced twist is very small in the root section of the blade, the steady state curvature (blue) together with the coupling induced twist (red) of the blade at 8 m/s wind speed is shown in Figure 6. For a bend-twist coupled blade the curvature, which for this example is largest in the outer part of the blade, has a significant influence on the twist. The curvature enters the beam strain vector of Equation 2 through $\frac{\partial\theta_1}{\partial z} = -\frac{\partial^2 u_2}{\partial z^2}$ and is coupled with the twist rate $\frac{\partial\theta_3}{\partial z}$ by the cross-section stiffness matrix. Reducing the cross-section constitutive relation of Equation 3 to flapwise curvature and twist and assuming torsion to be zero one obtains

$$\begin{bmatrix} K_{44} & K_{46} \\ K_{46} & K_{66} \end{bmatrix} \begin{Bmatrix} -\frac{\partial^2 u_2}{\partial z^2} \\ \frac{\partial\theta_3}{\partial z} \end{Bmatrix} = \begin{Bmatrix} M_1 \\ 0 \end{Bmatrix} \tag{8}$$

from which the following relationship between curvature and twist rate is obtained:

$$\frac{\partial\theta_3}{\partial z} = \frac{K_{46}}{K_{66}}\frac{\partial^2 u_2}{\partial z^2} \tag{9}$$

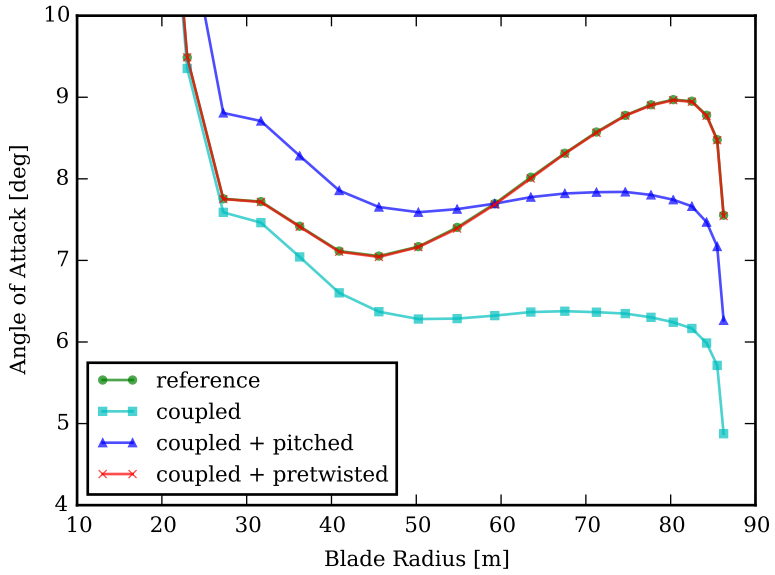

Figure 2: Angle of attack along the blade at 8 m/s wind speed for the uncoupled blade, the coupled ($\gamma = -0.2$) blade with the original pitch angle, the coupled blade with an optimized pitch angle and the coupled blade pretwisted at 8 m/s.

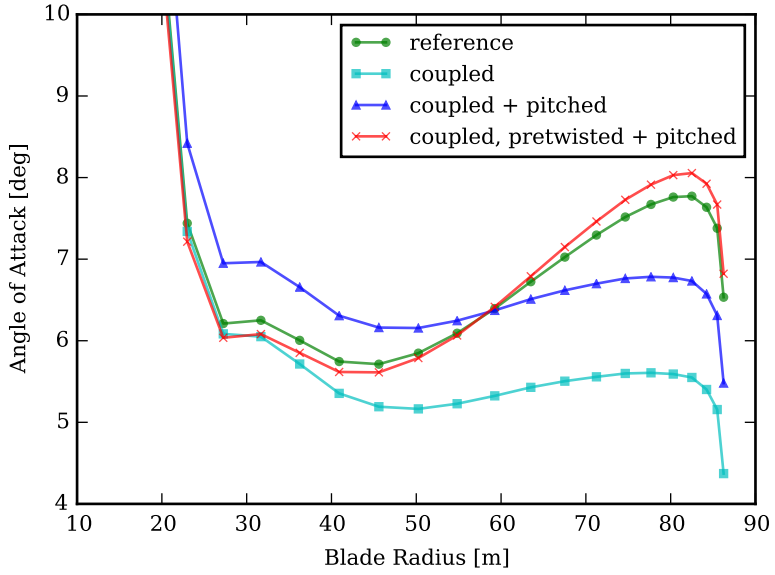

Figure 3: Angle of attack along the blade at 7 m/s wind speed for the uncoupled blade, the coupled ($\gamma = -0.2$) blade with the original pitch angle, the coupled blade with an optimized pitch angle and the coupled blade pretwisted at 8 m/s and optimal pitched.

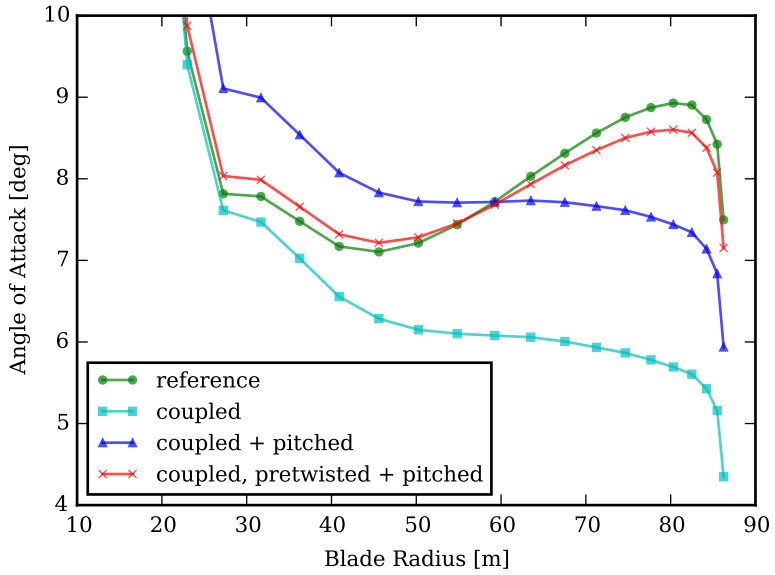

Figure 4: Angle of attack along the blade at 9 m/s wind speed for the uncoupled blade, the coupled ($\gamma = -0.2$) blade with the original pitch angle, the coupled blade with an optimized pitch angle and the coupled blade pretwisted at 8 m/s and optimal pitched.

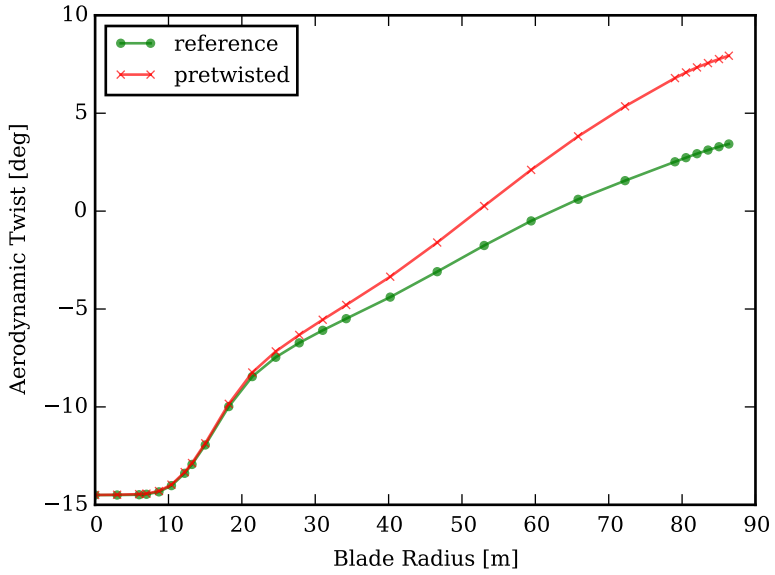

Figure 5: Aerodynamic twist along the blade for the reference blade and pretwisted blade at 8 m/s.

While the above relationship is a simplification ignoring nonlinear effects which are prevalent in anisotropic beams, it can serve as a first estimate of the blade twist. The curvature of Figure 6 results in a twist distribution where only 10% of the coupling induced tip twist is accumulated in the inner third of the blade. The middle third accounts for about 43% and the outer third for about 47% of the coupling induced tip twist. That coupling has only a small effect in the root region of the blade is also observed by Bottasso et al.[4] who report similar load alleviation for partially coupled blades compared to fully coupled blades. For material coupled blades, the change in fibre direction always results in a reduction of strength and stiffness in the principle beam direction. Due to the small curvature, coupling of the root region contributes little to the coupling induced twist of the blade investigated in this study. To improve strength and stiffness properties of bend-twist coupled blades it is therefore advisable to introduce coupling in regions with high curvature only.

Figure 7 shows the optimal pitch angle over wind speed for the reference blade (green), the coupled blade (blue) and the pretwisted blade (red). The coupled blade without pretwist requires a lower pitch angle to compensate for the coupling induced twist. For the pretwisted blade the pitch angle varies around the reference blade. Below the reference speed of 8 m/s the pitch angle is larger than for the reference turbine to compensate for the twist to stall due to lower thrust which is also observed in Figure 3. At reference speed the pitch angle of reference and pretwisted blade are equal. Between the reference speed of 8 m/s and a wind speed of about 13 m/s the pitch angle of the pretwisted blade is smaller to compensate for coupling induced twist to feather due to higher thrust. Above 13 m/s the thrust reduces again and a higher pitch angle is required to compensate for the twist to stall.

3.2 Annual Energy Production & Damage Equivalent Load Rate

Figure 8 shows the power curve (red) of the reference blade and the Rayleigh distribution with a mean wind speed of 10 m/s (blue) that was used for calculating the annual energy production. The relative difference of the power between the reference blade and the coupled (cyan), coupled and pitched (blue) and coupled, pretwisted and pitched blade (red) is shown in Figure 9. For low wind speeds, the coupled and the coupled and pitched blade show an increased energy capture. At low wind speeds the tip speed ratio is high ($\lambda = 14$ at 4 m/s) due to the minimum rotor speed (6 rpm) of the reference turbine. The blades that have not been pretwisted are twisted towards feather compared with the reference blade which results in a higher power coefficient along the blade. The pretwisted blade on the other hand is twisted towards stall compared with the reference blade which has a negative effect on the power. At about 7 m/s the tip speed ratio approaches the design tip speed ratio of the blade ($\lambda = 7.5$) and the pretwisted blade shows a better performance than the coupled only blades.

Figure 10 shows the change in AEP for 10 m/s mean wind speed from the reference blade over pretwist reference wind speed for different coupling coefficients. A mean wind speed of 10 m/s was considered to be representative for an offshore wind site. Alas, for a different mean wind speed the results will differ quantitatively. On average the best performance is achieved when the blade is pretwisted at 8 m/s. In this study, the reference speed for pretwisting was therefore chosen as 8 m/s. Figure 11 shows the effect of bend-twist coupling on the annual energy production and blade root flapwise moment damage equivalent load rate for a coupled blade with optimal pitch (blue) and a pretwisted blade (red). The power loss of the coupled blade follows a parabolic curve while the pretwisted blade has a linear relationship between AEP and coupling. The figure shows that the power loss associated with bend-twist coupled blades can be reduced significantly if the twist distribution of the blade is adjusted for the coupling induced twist. The relationship of damage equivalent load rate and coupling coefficient is close to linear for both blades. Also, there is no significant difference between the load alleviation capabilities of the coupled and the coupled and pretwisted blade.

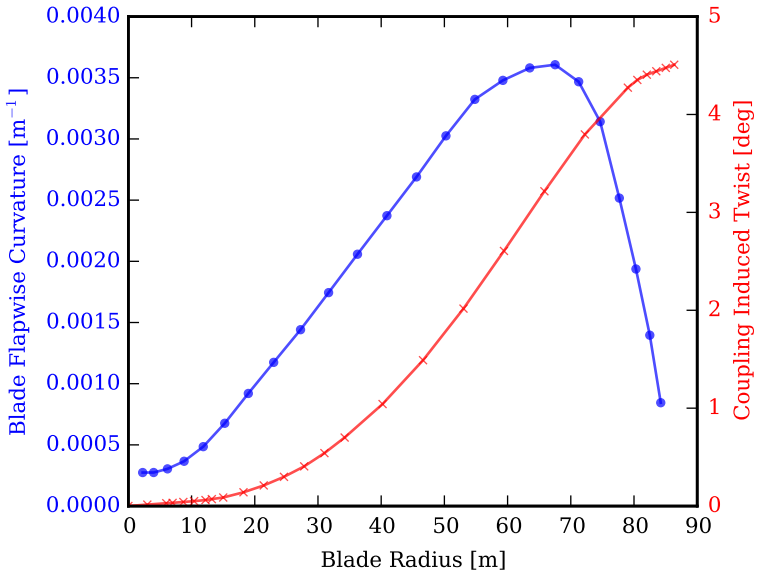

Figure 6: Blade flapwise steady state curvature and coupling induced twist at 8 m/s wind speed.

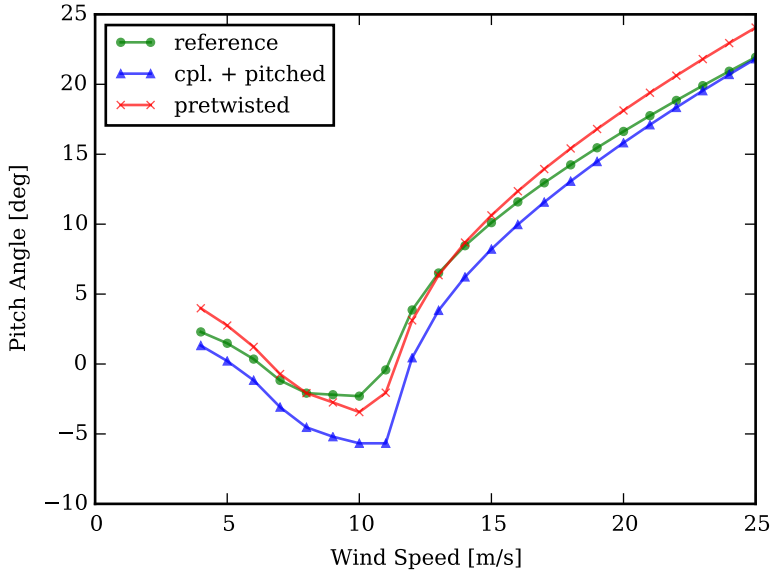

Figure 7: Optimal pitch angle over wind speed for the reference blade (green), the coupled blade (blue) and the pretwisted blade (red).

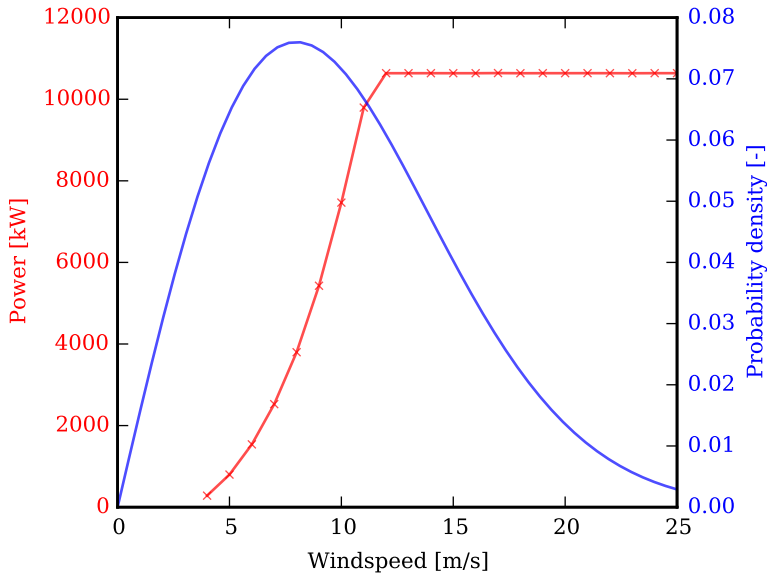

Figure 8: Power curve of the reference turbine and Rayleigh distribution (10 m/s mean) used for AEP calculation.

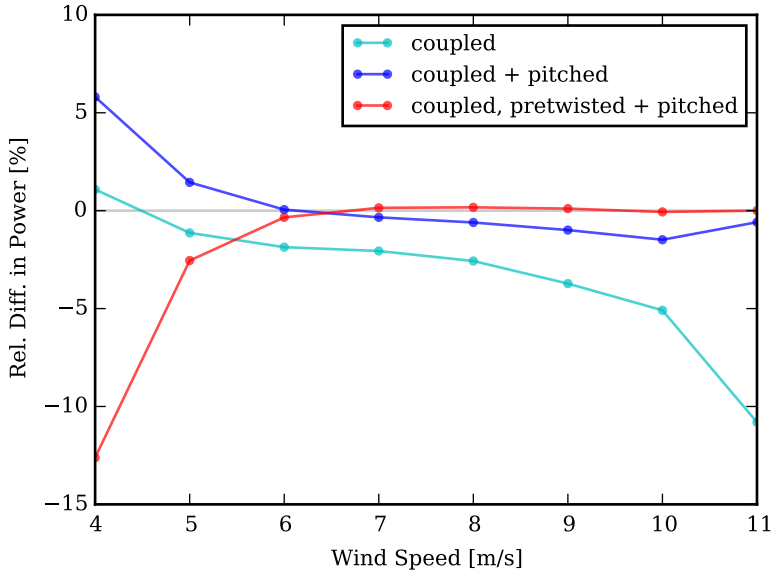

Figure 9: Relative difference in power between the reference blade and the coupled (cyan), coupled and pitched (blue) and coupled, pretwisted and pitched blade (red). The coupling coefficient of all blades is $\gamma = -0.2$ twisting to feather.

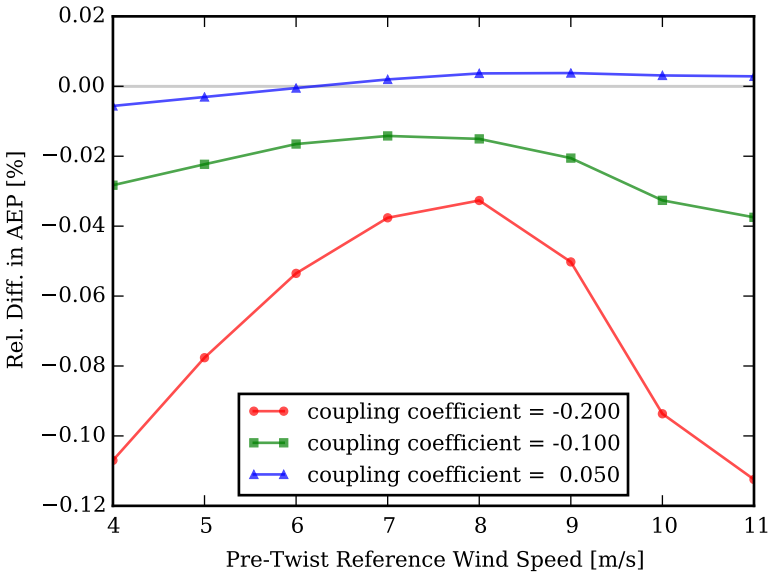

Figure 10: Change in AEP for 10 m/s mean wind speed from the reference blade over pretwist reference wind speed for different coupling coefficients.

3.3 Conclusion

The effect of pretwisting on the annual energy production and damage equivalent load rate of the bend-twist coupled DTU 10 MW Reference Wind Turbine blade was investigated in this study. The steady state properties of the turbine were obtained by means of the blade element momentum theory and a nonlinear beam model that allows for anisotropic cross-sectional properties. To compensate for the coupling induced twist, a pretwisting procedure suitable for large blade deflections has been introduced. The damage equivalent load rate was evaluated by obtaining the power spectral density of the turbine response to wind input in the frequency domain and applying a spectral method. It was shown that the pretwisting procedure results in an equal angle of attack along the blade at the pretwist reference wind speed. The pretwist obtained with the procedure confirmed previous studies that showed little effect of blade coupling in the inner third of the blade. It was shown that the coupling induced twist depends on the curvature of the blade and it was suggested that coupling should only be introduced in blade regions with increased curvature. The annual energy production seems to depend quadratic on the coupling coefficient if the twist is not adjusted. For pretwisted blades the coupling-AEP dependency seems linear. Damage equivalent load rate depends close to linear on the coupling coefficient and is influenced only little by pretwisting.

The approach to determine the twist distribution of coupled blades presented in this paper does not necessarily provide an optimal power coefficient and further improvements could be made by determining an optimal twist distribution for coupled blades. Such an optimal twist distribution might not necessarily yield optimal results at any operational point but provide a better overall performance. It would also be interesting to validate the effects of pretwist on AEP and fatigue load under non-uniform inflow and with different turbulence intensities.

Acknowledgement

The present work is funded by the European Commision under the programme ‘FP7-PEOPLE-2012-ITN Marie Curie Initial Training Networks’ through the project ‘MARE-WINT - new MAterials and REliability in offshore WINd Turbines technology’, grant agreement no. 309395.

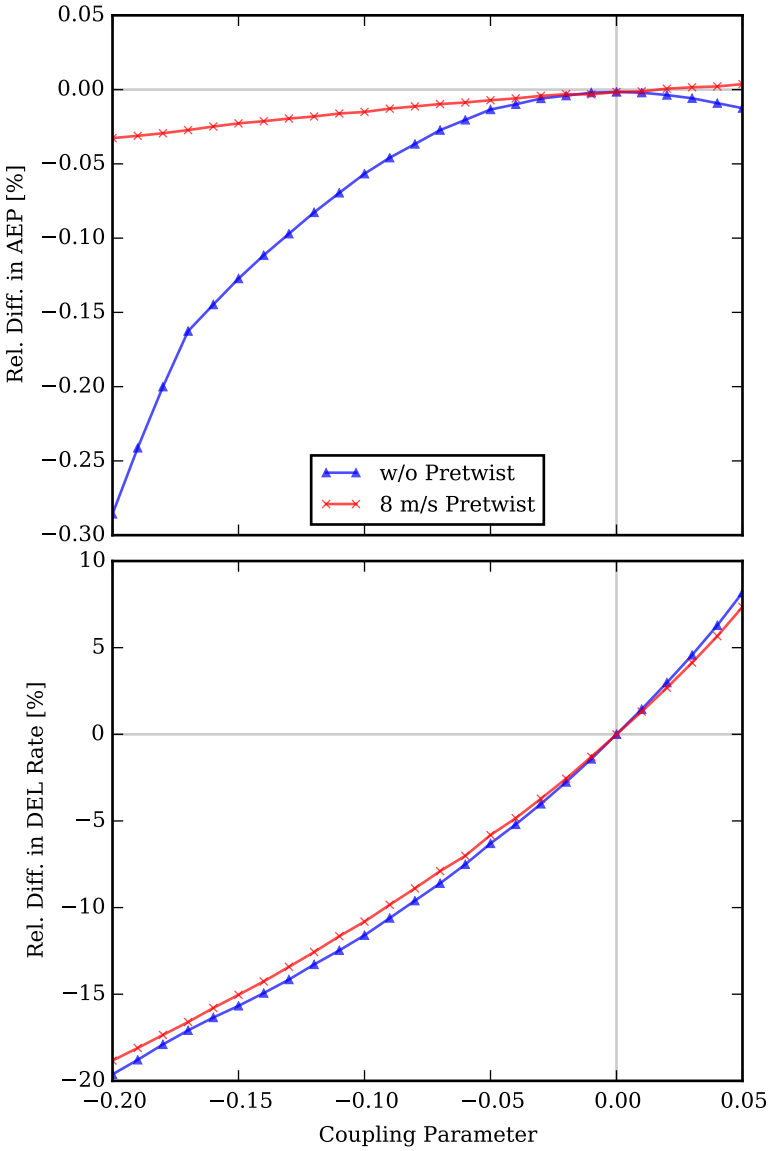

Figure 11: Effect of bend-twist coupling on the annual energy production and blade root flapwise moment damage equivalent load rate for a coupled blade with optimal pitch and a pretwisted blade.

References

[1] Lobitz, D. W. and Veers, P. S., "Load Mitigation with Bending/Twist-coupled Blades on Rotors using Modern Control Strategies," *Wind Energy*, Vol. 6, No. 2, 2003, pp. 105–117, DOI: 10.1002/we.74.

[2] Verelst, D. R. and Larsen, T. J., "Load Consequences When Sweeping Blades - A Case Study of a 5 MW Pitch Controlled Wind Turbine," Tech. Rep. Risø-R-1724(EN), Risø National Laboratory for Sustainable Energy, 2010.

[3] Lobitz, D. W. and Laino, D. J., "Load Mitigation with Twist-Coupled HAWT Blades," *ASME/AIAA Wind Energy Symposium, Reno, NV*, 1999, pp. 124–134, DOI: 10.2514/6.1999-33.

[4] Bottasso, C. L., Campagnolo, F., Croce, A., and Tibaldi, C., "Optimization-Based Study of Bend–Twist Coupled Rotor Blades for Passive and Integrated Passive/Active Load Alleviation," *Wind Energy*, Vol. 16, No. 8, 2013, pp. 1149–1166, DOI: 10.1002/we.1543.

[5] Henriksen, L. C., Tibaldi, C., and Bergami, L., "HAWCStab2 User Manual," Tech. rep., DTU Wind Energy, Sept. 2014.

[6] Stäblein, A. R. and Hansen, M. H., "Timoshenko Beam Element with Anisotropic Cross-Sectional Properties," *To be submitted.*.

[7] Lobitz, D. W. and Veers, P. S., "Aeroelastic Behavior of Twist-Coupled HAWT Blades," *ASME/AIAA Wind Energy Symposium, Reno, NV*, 1998, pp. 75–83, DOI: 10.2514/6.1998-29.

[8] Tibaldi, C., Henriksen, L. C., Hansen, M. H., and Bak, C., "Wind Turbine Fatigue Damage Evaluation Based on a Linear Model and a Apectral Method," *Wind Energy*, 2015, DOI: 10.1002/we.1898.

[9] Hansen, M. H., "Aeroelastic Properties of Backward Swept Blades," *Proceedings of 49th AIAA Aerospace Sciences Meeting Including The New Horizons Forum and Aerospace Exposition, Orlando*, 2011, pp. 4–7, DOI: 10.2514/6.2011-260.

[10] Sønderby, I. and Hansen, M. H., "Open-Loop Frequency Response Analysis of a Wind Turbine Using a High-Order Linear Aeroelastic Model," *Wind Energy*, Vol. 17, No. 8, 2014, pp. 1147–1167, DOI: 10.1002/we.1624.

[11] Morten H. Hansen et al., "The Linear Aero-Servo-Elastic Code HAWCStab2," Tech. rep., DTU Wind Energy, To be published.

[12] Giavotto, V., Borri, M., Mantegazza, P., Ghiringhelli, G. L., Carmaschi, V., Maffioli, G. C., and Mussi, F., "Anisotropic Beam Theory and Applications," *Computers & Structures*, Vol. 16, No. 1, 1983, pp. 403–413, DOI: 10.1016/0045-7949(83)90179-7.

[13] Hodges, D. H., *Nonlinear Composite Beam Theory*, American Institute of Aeronautics and Astronautics, Reston, Va., 2006.

[14] Blasques, J. P., "BECAS - A Cross Section Analysis Tool for Anisotropic and Inhomogeneous Beam Sections of Arbitrary Geometry," Tech. Rep. Risø-R-1785(EN), Risø National Laboratory for Sustainable Energy, 2011.

[15] Cesnik, C. E. S. and Hodges, D. H., "VABS: A New Concept for Composite Rotor Blade Cross-Sectional Modeling," *Journal of the American Helicopter Society*, Vol. 42, No. 1, 1997, pp. 27–38, DOI: 10.4050/JAHS.42.27.

[16] Larsen, T. J. and Hansen, A. M., "How 2 HAWC2, The User's Manual," Tech. Rep. Risø-R-1597(ver. 4-5)(EN), Risø National Laboratory for Sustainable Energy, July 2014.

[17] Benasciutti, D. and Tovo, R., "Spectral Methods for Lifetime Prediction Under Wide-Band Stationary Random Processes," *International Journal of Fatigue*, Vol. 27, No. 8, 2005, pp. 867–877, DOI: 10.1016/j.ijfatigue.2004.10.007.

[18] Benasciutti, D. and Tovo, R., "Comparison of Spectral Methods for Fatigue Analysis of Broad-Band Gaussian Random Processes," *Probabilistic Engineering Mechanics*, Vol. 21, No. 4, 2006, pp. 287–299, DOI: 10.1016/j.probengmech.2005.10.003.

[19] Bak, C., Zahle, F., Bitsche, R., Kim, T., Yde, A., Henriksen, L. C., Natarajan, A., and Hansen, M. H., "Description of the DTU 10 MW Reference Wind Turbine," Tech. Rep. DTU Wind Energy Report-I-0092, DTU Wind Energy, 2013.

[20] "The DTU 10MW Reference Wind Turbine Project Site," http://dtu-10mw-rwt.vindenergi.dtu.dk.